MOLECULAR AND CELLULAR BIOLOGY, Nov. 2007, p. 7582–7593 Vol. 27, No. 21
0270-7306/07/$08.00+0 doi:10.1128/MCB.00493-07

G Protein-Coupled Receptor Ca^{2+}-Linked Mitochondrial Reactive Oxygen Species Are Essential for Endothelial/Leukocyte Adherence▽†

Brian J. Hawkins,[1,5] Laura A. Solt,[2] Ibrul Chowdhury,[1] Altaf S. Kazi,[1] M. Ruhul Abid,[3] William C. Aird,[3] Michael J. May,[2] J. Kevin Foskett,[4] and Muniswamy Madesh[1,5]*

Institute for Environmental Medicine, University of Pennsylvania, Philadelphia, Pennsylvania 19104[1]; Department of Animal Biology, School of Veterinary Medicine, University of Pennsylvania, Philadelphia, Pennsylvania 19104[2]; Department of Medicine, Beth Israel Deaconess Medical Center and Harvard Medical School, Boston, Massachusetts[3]; Department of Physiology, University of Pennsylvania, Philadelphia, Pennsylvania 19104[4]; and Department of Cancer Biology, University of Pennsylvania, Philadelphia, Pennsylvania 19104[5]

Received 21 March 2007/Returned for modification 20 June 2007/Accepted 16 August 2007

Receptor-mediated signaling is commonly associated with multiple functions, including the production of reactive oxygen species. However, whether mitochondrion-derived superoxide (mROS) contributes directly to physiological signaling is controversial. Here we demonstrate a previously unknown mechanism in which physiologic Ca^{2+}-evoked mROS production plays a pivotal role in endothelial cell (EC) activation and leukocyte firm adhesion. G protein-coupled receptor (GPCR) and tyrosine kinase-mediated inositol 1,4,5-trisphosphate-dependent mitochondrial Ca^{2+} uptake resulted in NADPH oxidase-independent mROS production. However, GPCR-linked mROS production did not alter mitochondrial function or trigger cell death but rather contributed to activation of NF-κB and leukocyte adhesion via the EC induction of intercellular adhesion molecule 1. Dismutation of mROS by manganese superoxide dismutase overexpression and a cell-permeative superoxide dismutase mimetic ablated NF-κB transcriptional activity and facilitated leukocyte detachment from the endothelium under simulated circulation following GPCR- but not cytokine-induced activation. These results demonstrate that mROS is the downstream effector molecule that translates receptor-mediated Ca^{2+} signals into proinflammatory signaling and leukocyte/EC firm adhesion.

A common mechanism in which external stimuli evoke Ca^{2+} signaling is through receptor-mediated pathways that involve the second messenger inositol 1,4,5-trisphosphate ($InsP_3$). Once generated by phospholipases, $InsP_3$ binds to $InsP_3$ receptors ($InsP_3R$) on the endoplasmic reticulum to trigger Ca^{2+} release. During normal signaling, $InsP_3R$-mediated Ca^{2+} transients may be transmitted to the mitochondria, raising mitochondrial matrix Ca^{2+} and enhancing mitochondrial bioenergetics (26, 63). However, excess Ca^{2+} can lead to mitochondrial Ca^{2+} overload, mitochondrial dysfunction, and apoptosis (5, 44, 55). Ca^{2+} mobilization and subsequent uptake by mitochondria is also correlated with an increase in mitochondrion-derived superoxide (mROS) production (10). However, whether mROS production during Ca^{2+}-mediated signaling participates directly in physiologic signaling cascades or occurs simply as a by-product of enhanced mitochondrial respiration is unclear.

In response to injury, endothelial cells (ECs) recruit circulating leukocytes to facilitate wound healing (9). Intercellular adhesion molecules (ICAMs) and vascular cell adhesion molecule 1 (VCAM-1) are immunoglobulin superfamily vascular ligands that specifically interact with leukocyte integrin receptors to arrest circulating leukocytes (8, 57). Leukocyte affinity for ECs is enhanced locally and rapidly by endothelium-derived chemokines (11, 24). However, little is known about the signaling events in ECs that cause rolling leukocytes to adhere firmly to endothelial monolayers that have been activated by G protein-coupled receptor (GPCR) agonists such as thrombin. Although it has been suggested that GPCR signaling events contribute to leukocyte firm adherence, it has been difficult to separate these events from the response to leukocyte chemotactic signals (11, 24).

In this study, we designed an ex vivo model in which thrombin-activated pulmonary microvascular ECs (PMVECs) were overlaid with unstimulated leukocytes to assess the role of EC activation in leukocyte firm adhesion under conditions of simulated circulation. We discovered that GPCR-linked mROS production is the key factor for activation of NF-κB-triggered EC adhesion molecule expression and leukocyte firm adherence. Thrombin-induced, $InsP_3R$-mediated Ca^{2+} signals were transmitted to mitochondria and stimulated the production of mROS. Prevention of $InsP_3R$-linked mitochondrial Ca^{2+} uptake attenuated mROS production and inhibited endothelial activation via NF-κB. Furthermore, the tight interaction between leukocytes and endothelial layers was inhibited by a reactive oxygen species (ROS) scavenger. These effects were specific for mROS, since similar effects were observed in cells that lacked the NADPH oxidase subunit $gp91^{phox}$. Unlike GPCR-linked signaling, tumor necrosis factor alpha (TNF-α) triggered NF-κB activation, ICAM-1 expression, and leukocyte/EC adherence independently of mROS. Our study demonstrates that GPCR-linked Ca^{2+} signals exquisitely modulate

* Corresponding author. Mailing address: Institute for Environmental Medicine, University of Pennsylvania, 3620 Hamilton Walk, One John Morgan Building, Philadelphia, PA 19104-6068. Phone: (215) 898-2095. Fax: (215) 898-0868. E-mail: madeshm@mail.med.upenn.edu.

† Supplemental material for this article may be found at http://mcb.asm.org/.

▽ Published ahead of print on 27 August 2007.

vascular activation via mROS production by ECs, thus suggesting that mROS signaling might promote rapid targeting of circulating leukocytes to sites of acute inflammation.

MATERIALS AND METHODS

Cells and cell culture. Murine PMVECs (MPMVECs) isolated from lungs as previously described (47) were cultured in Dulbecco's modified Eagle medium (DMEM) supplemented with 10% fetal calf serum (FCS), nonessential amino acids, and antibiotics. Human PMVECs (HPMVECs) were cultured in M199 supplemented with 15% FCS, L-glutamine, and antibiotics. Wild-type DT40 (DT40 WT) and triple-$InsP_3R$-knockout (DT40 TKO) B-cell lines were cultured in RPMI 1640 supplemented with 10% FCS, 1% chicken serum, and antibiotics. J774.1 macrophages were cultured in RPMI 1640 supplemented with 10% FCS and antibiotics. Primary cells were used between passages 6 and 20.

Simultaneous measurements of cytosolic free Ca^{2+} concentration ($[Ca^{2+}]_i$) mobilization and mitochondrial Ca^{2+} uptake. MPMVECs were loaded with 2 μM Rhod-2/AM (Invitrogen, Carlsbad, CA) in extracellular medium (ECM) containing 2.0% bovine serum albumin (BSA) at 37°C for 50 min. Rhod-2-loaded cells were washed and loaded with the cytosolic Ca^{2+} indicator Fluo-4/AM (5 μM; Invitrogen, Carlsbad, CA) for an additional 30 min at room temperature. Cells were then placed in ECM containing 0.25% BSA on a temperature-controlled stage and images recorded every 3 s using the Bio-Rad Radiance 2000 imaging system (Bio-Rad Laboratories, Hercules, CA) equipped with a Kr/Ar-ion laser source with excitation at 488 nm and 568 nm for Fluo-4 and Rhod-2, respectively, using a Nikon TE3000 inverted microscope with a 60× oil objective. Thrombin was added following 0.5 min of baseline recording. Ca^{2+} chelation experiments were conducted by preincubation with 25 μM 1,2-bis(O-aminophenoxy)ethane-*N*,*N*,*N*′,*N*′,-tetraacetic acid acetoxymethyl aster (BAPTA/AM) for 20 min and hirudin (Hir) inhibition (1 U/ml) as described above. Tracings are representative of the mean cellular response of three to five independent experiments and obtained by nuclear masking for Fluo-4 and perinuclear masking for Rhod-2 fluorescence (Spectralyzer, custom software). All confocal methodologies have been published previously in greater detail (28, 44).

Simultaneous assessment of $[Ca^{2+}]_i$ and mROS production. To visualize mROS production, MPMVECs and DT40 WT and TKO cells affixed to 0.2% gelatin and Cell-Tak (BD Biosciences, San Jose, CA)-coated coverslips, respectively, were loaded with the mitochondrial $O_2{\cdot}^-$-sensitive fluorophore MitoSOX Red (Invitrogen; 10 μM) in ECM containing 2% BSA at 37°C for 10 min. Cells were then incubated with Fluo-4/AM for an additional 20 min at room temperature. MPMVECs were then washed, resuspended in ECM containing 0.25% BSA, placed on a temperature-controlled stage, and imaged every 3 s at 488 nm and 568 nm for Fluo-4 and MitoSOX Red, respectively, as described above. Thrombin and ionomycin (Iono) were added following 0.5 min of baseline recording. Ruthenium red (RR) (Calbiochem) was added to MPMVECs throughout loading and imaging to inhibit mitochondrial Ca^{2+} uptake. Tracings are obtained similarly to those for Fluo-4 and Rhod-2.

Measurement of $[Ca^{2+}]_i$ and $\Delta\psi_m$. MPMVECs were loaded with Fluo-4/AM and tetramethylrhodamine ethyl ester perchlorate (TMRE) (100 nM) for $[Ca^{2+}]_i$ and $\Delta\psi_m$ measurement, respectively. Images are recorded every 5 s using confocal microscopy. Upon changes in $\Delta\psi_m$, TMRE dissociates from the mitochondria and can be detected in the nucleus.

ROS measurement. PMVECs cultured on 25-mm-diameter glass coverslips were loaded with the $O_2{\cdot}^-$-sensitive dye hydroethidine (HE) (10 μM) in DMEM for 10 min at 37°C. Cells were then placed on a temperature-controlled stage and images recorded every 5 s for 10 min using confocal microscopy. Antimycin A (AA) (2 μM) and thrombin (500 mU/ml) were added following 1 min of baseline recording.

Adenoviral infection. Studies used similar multiplicities of infection to test the recombinant adenoviral manganese superoxide dismutase (MnSOD) vector (Ad5CMVSOD2; University of Iowa Gene Transfer Vector Core). Both MPMVECs and HPMVECs were subjected to adenoviral infection at a multiplicity of infection of 2,000 particles/cell, which resulted in greater MnSOD transduction as evidenced by protein expression (see Fig. S4 in the supplemental material).

Electron microscopy. MPMVECs were serum starved in DMEM containing 0.5% fetal bovine serum overnight and then incubated in serum-free DMEM for 1 h prior to treatment with 1.0 U/ml thrombin alone or thrombin inactivated by 2.0 U/ml Hir. Cells were washed twice in phosphate-buffered saline (PBS), trypsinized, resuspended in fixative containing ice-cold 5% glutaraldehyde in 0.1 M sodium cacodylate buffer, pH 7.4, at 4°C for 15 min, and then centrifuged. Cell pellets were then continuously fixed for 4 h. After a complete rinse with sodium cacodylate buffer, the cell pellet was further fixed in 1% OsO_4 in 0.1 M sodium cacodylate buffer on ice for 1 h and dehydrated with acetone. Cell pellet was embedded in EM-bed 812 resin and polymerized at 60°C for 48 h. A Leica Ultracut UCT ultramicrotome (Vienna, Austria) was used to cut ultrathin sections (70 nm) that were counterstained with uranyl acetate and lead citrate. Images were collected using a JEOL electron microscope, model 100 CX (Tokyo, Japan), equipped with a Hamamatsu camera.

Confocal imaging of apoptotic markers. To assess apoptosis, cells were incubated with the conjugate annexin V Alexa Fluor-595 (Invitrogen) and TOTO-3 (0.5 μg/ml) for 15 min. Untreated cells and cells following treatment with 1 U/ml thrombin or the superoxide generating system (100 μM xanthine plus 20 mU/ml xanthine oxidase) were visualized at 6 h and 4 h, respectively, for annexin V and TOTO-3 via confocal microscopy at 568 nm and 647 nm, respectively.

Electrophoretic mobility shift assay. HPMVECs were incubated with or without 50 μM Mn(III) tetrakis (y-benzoic acid) porphyrin (MnTBAP) or 25 μM BAPTA/AM. Thrombin (0.5 U/ml), TNF-α (10 ng/ml), or AA (20 μM) was added for 90 min, and cells were pelleted and nuclear extracts prepared. Single-stranded complementary oligonucleotides encompassing a consensus NF-κB site (upper strand, 5′-AGTTGAGGGGACTTTCCCAGGC-3′) or the Oct-1 probe (Santa Cruz) were annealed and then labeled with [γ-^{32}P]ATP using T4 polynucleotide kinase (New England Biolabs, Beverly, MA). Labeled probe was purified using mini-Quick Spin columns (Roche) according to manufacturer's instructions. For the electrophoretic mobility shift assay, 2 to 5 μg of nuclear extracts supplemented with 1 μg of poly(dI/dC) (Roche) were incubated with an equal volume of 2× binding buffer (40 mM Tris · Cl [pH 7.9], 100 mM NaCl, 10 mM $MgCl_2$, 2 mM EDTA, 20% glycerol, 0.2% NP-40, 2 mM dithiothreitol, 100 μg/ml BSA) on ice for 10 min. After incubation, 1 μl of labeled probe was added and samples incubated at room temperature for 20 min. Resulting DNA–NF-κB complexes were separated on 5% polyacrylamide nondenaturing gels by electrophoresis.

NF-κB luciferase activity. Confluent HPMVECs (5×10^6) were transfected with 3 μg of pNF-κB-Luc (Clontech, Palo Alto, CA) and 3 μg of pSV-β-galactosidase control vector (Promega) to normalize transfection efficiencies. Appropriate positive (pGL3-control) and negative (pGL3-basic) vectors were included to verify reporter activity. After transfection, HPMVECs were cultured and incubated for 1 h in serum-free M199 with or without 50 μM MnTBAP or 25 μM BAPTA/AM. Thrombin (500 mU/ml), TNF-α (10 ng/ml), and AA (20 μM) were added, and the cells were incubated for 7 h, washed twice with PBS, and lysed in 150 μl of the reporter lysis buffer according to the manufacturer's instructions (Promega). Cell debris was removed and the supernatant used in the luciferase assay using a TD-20/20 luminometer (Turner Designs, Sunnyvale, CA).

Immunoblotting. HPMVECs were incubated for 1 h in serum-free M199 with or without 50 μM MnTBAP, 25 μM BAPTA, or MG132 (3 μM). Thrombin (1.0 U/ml), TNF-α (10 ng/ml), and AA (20 μM) were added and cultured for 6 h. MPMVECs were washed twice with PBS and lysed in RIPA buffer (Upstate Biotechnology, Inc.). Proteins were separated and probed for ICAM-1 (Santa Cruz Biotechnology, Santa Cruz, CA) according to standard protocols. DT40 lysates were separated and probed for mitochondrial OxPhos complexes I (NADH dehydrogenase subunit 20 kDa) and IV (cytochrome *c* oxidase subunit 1) proteins (MitoSciences, Eugene, OR) and $InsP_3R$ type 3 isoform (BD Transduction Laboratories).

Leukocyte adhesion. HPMVECs in complete medium were plated on a glass slide (44 by 20 mm) coated with 0.2% gelatin. Cells were cultured for 24 h until ~90% confluent and were then incubated with MnTBAP (50 μM) for 1 h and stimulated with thrombin (500 mU/ml) or TNF-α (10 ng/ml) for 12 h. For ICAM-1 blocking studies, thrombin-stimulated PMVECs were incubated with mouse monoclonal (B-H17) antibody to ICAM1 (ab34319; Abcam, Cambridge, MA) for 30 min prior to addition of J774.1. Mouse immunoglobulin G (IgG) was used as a negative control. HPMVECs were labeled with Cell Tracker Red (1 μM; Invitrogen) for 15 min, washed twice, resuspended in serum-free medium, and mounted in the RC-30 confocal imaging chamber (Warner Instruments, Hamden, CT). J774.1 macrophages were labeled with Cell Tracker Green (1 μM) using a similar procedure and resuspended in complete medium. Macrophages (5×10^5) were evenly added onto HPMVECs and allowed to adhere for 5 min. The chamber was then sealed and shear stress introduced to the chamber via circulation of ~20 ml of medium. Shear stress (τ) was calculated as follows: $\tau = (6\mu/bh^2)\dot{Q}$, where μ is viscosity, *b* and *h* are flow chamber width and height, respectively, and $\dot{Q}$ is the flow rate (ml/min). The initial flow rate was 1.5 dynes/cm^2, which was increased to 2.5 dynes/cm^2 after 1 min for an additional 5 min. The total time HPMVECs were exposed to flow was 6 min. Cell Tracker Green-labeled J774.1 macrophages and Cell Tracker Red-labeled HPMVECs were imaged before and after shear stress at 488 nm and 568 nm, respectively, using a 60× oil objective. Following application of shear stress, nine additional

random fields were chosen for three to four independent experiments and J774.1 cells quantified.

Data analysis. Unless indicated as single-cell recording, tracings are representative of the mean fluorescence value of all cells in one field normalized to the baseline level and are indicative of three to six independent experiments. Results of multiple experiments were quantified to determine peak *n*-fold change, expressed as the mean ± standard error of the mean for three to six independent experiments.

RESULTS

PAR1 regulates thrombin-triggered mitochondrial Ca^{2+} pool size rise. Thrombin is a multifunctional serine protease that activates ECs via protease-activated receptors (PARs) (14). Upon thrombin activation, PARs mediate Ca^{2+} mobilization through phospholipase C and the generation of the second messenger $InsP_3$ (15). MPMVECs exposed to thrombin demonstrated a dose-dependent rapid rise of $[Ca^{2+}]_i$ that was blocked by the competitive inhibitor Hir (2.0 U/ml) (see Fig. S1A and D in the supplemental material). Thrombin activates PAR by cleaving the receptor amino terminus, exposing a peptide sequence that serves as a self-activating "tethered ligand" (42). Previously it was shown that thrombin triggered Ca^{2+} mobilization through PAR1 and PAR4 (34). Application of the specific PAR1 agonist (SFLLRN-amide) caused a dose-dependent rapid $[Ca^{2+}]_i$ elevation that was similar to that observed in response to thrombin (see Fig. S1B in the supplemental material), whereas Ca^{2+} mobilization was not observed following application of the PAR4-specific peptide agonist (GYPGKF-amide). Thus, thrombin leads to rapid $[Ca^{2+}]_i$ mobilization in PMVECs via the GPCR PAR1. In response to elevated $[Ca^{2+}]_i$, Ca^{2+} can be sequestered into mitochondria, where it elicits varied responses (4, 31). Exposure to 500 mU/ml thrombin caused a rapid increase in mitochondrial Ca^{2+} concentration that immediately followed the rise of $[Ca^{2+}]_i$ (Fig. 1A and B). A lower level of thrombin (1 mU/ml) also raised $[Ca^{2+}]_i$ and subsequently increased mitochondrial $[Ca^{2+}]$ (Fig. 1C), although to a lesser extent than that observed with the higher dose (500 mU/ml). Interestingly, the low level of agonist produced heterogenous responses among cells in both cytosolic and mitochondrial $[Ca^{2+}]$ (see Fig. S2A in the supplemental material). Of note, mitochondrial Ca^{2+} uptake (see Fig. S2C in the supplemental material) was directly proportional to the magnitude of the cytosolic $[Ca^{2+}]$ (see Fig. S2B in the supplemental material). Both inhibition of thrombin by Hir and chelation of intracellular Ca^{2+} by BAPTA completely eliminated both the cytosolic $[Ca^{2+}]$ transient (Fig. 2D) and mitochondrial Ca^{2+} uptake (Fig. 1E).

GPCR-linked mitochondrial Ca^{2+} uptake triggers mROS production. Under normal conditions, $InsP_3R$-mediated Ca^{2+} release that is transmitted to the mitochondria stimulates mitochondrial bioenergetics (NADH production) to generate ATP (63). Accordingly, the increase in electron transport enzyme activity is likely coupled to increased formation of mROS (58), which can be released into the cytoplasm through the voltage-dependent anion channel (27, 43). We therefore considered whether receptor-mediated Ca^{2+} signals that are transmitted to the mitochondria may in turn lead to mROS generation. MPMVECs were loaded with the Ca^{2+} indicator dye Fluo-4 and the mitochondrial superoxide ($O_2\cdot^-$) indicator MitoSOX Red (28, 48) to simultaneously assess the kinetics of $[Ca^{2+}]_i$ and mROS generation in response to thrombin. Thrombin-induced elevation of $[Ca^{2+}]_i$ caused enhanced mROS production (Fig. 2A and B) even at low concentrations (1 mU/ml) (Fig. 2C). Thus, even submaximal mitochondrial Ca^{2+} uptake (refer to Fig. 1C) is associated with enhanced mROS generation. This increase in mROS production is mainly dependent on elevated $[Ca^{2+}]_i$, since thrombin inhibition by Hir completely blocked the changes in MitoSOX Red fluorescence (Fig. 2D), and mROS production was stimulated by the Ca^{2+} ionophore Iono (Fig. 2E). Ca^{2+} uptake by mitochondria is mediated by a ruthenium red (RR)-sensitive uptake mechanism in the mitochondrial inner membrane (36). Inhibition of mitochondrial Ca^{2+} uptake by pretreatment of cells with RR suppressed mROS generation in a dose-dependent fashion (Fig. 2F). To exclude the possibility that thrombin stimulated mROS production through NADPH oxidase, mROS was measured in response to thrombin in MPMVECs lacking the catalytic subunit of the NADPH oxidase complex, $gp91^{phox-/-}$. MPMVECs lacking $gp91^{phox-/-}$ also displayed thrombin-induced mROS production (Fig. 2G). It is important to note the transient profile of MitoSOX Red fluorescence in $gp91^{phox-/-}$ cells stimulated with thrombin. A transient MitoSOX Red fluorescence profile indicates dissociation of the dye from the mitochondria secondary to alterations in mitochondrial membrane potential. The MitoSOX Red fluorescence profile suggests that $gp91^{phox-/-}$ cells are more sensitive to a rise in $[Ca^{2+}]_i$ and may constitute an important phenotype in NADPH oxidase knockout mice. Pretreatment with the flavin-dependent NADPH oxidase inhibitor diphenyleneiodonium (DPI) (10 μM) did not reduce MitoSOX Red fluorescence (Fig. 2I). To further verify whether mitochondria are the source of Ca^{2+}-dependent $O_2\cdot^-$ production, thrombin-stimulated MitoSOX Red fluorescence was abolished by overexpression of MnSOD (Fig. 2H). Studies have proposed that stigmatellin inhibits mitochondrial $O_2\cdot^-$ production at the Q_0 site of respiratory complex III (2, 49). Pretreatment with stigmatellin (2 μM) effectively inhibited mROS production (Fig. 2I). Thus, thrombin causes a dose-dependent increase in mROS production that is facilitated by mitochondrial Ca^{2+} uptake, consistent with Ca^{2+} stimulation of oxidative phosphorylation and concomitant ROS production (Fig. 2I).

NADPH oxidase-independent mROS production is $InsP_3R$ dependent. A rapid enhancement of mROS was observed in the mean response of DT40 chicken pre-B WT cells in response to B-cell receptor (BCR) cross-linking (Fig. 3B). mROS accumulation was evident after two to three $[Ca^{2+}]_i$ oscillations (Fig. 3A), indicating a mitochondrial Ca^{2+} threshold needed to induce mROS production. Like WT cells, DT40 cells lacking all three isoforms of the $InsP_3R$ (TKO) possess the mitochondrial machinery necessary for electron transport and associated mROS formation (Fig. 3C). Nevertheless, anti-IgM-dependent mROS production was completely abolished in TKO cells (Fig. 3D), demonstrating that $InsP_3R$-mediated $[Ca^{2+}]_i$ elevation is necessary for mROS production. The $[Ca^{2+}]_i$ rise in B cells upon BCR cross-linking occurs in two distinct phases, release from the endoplasmic reticulum intracellular stores and subsequent Ca^{2+} entry across the plasma membrane (52). However, stimulation of WT cells in the presence of the extracellular Ca^{2+} chelator EGTA did not prevent mROS production (Fig. 3E), suggesting that Ca^{2+} released

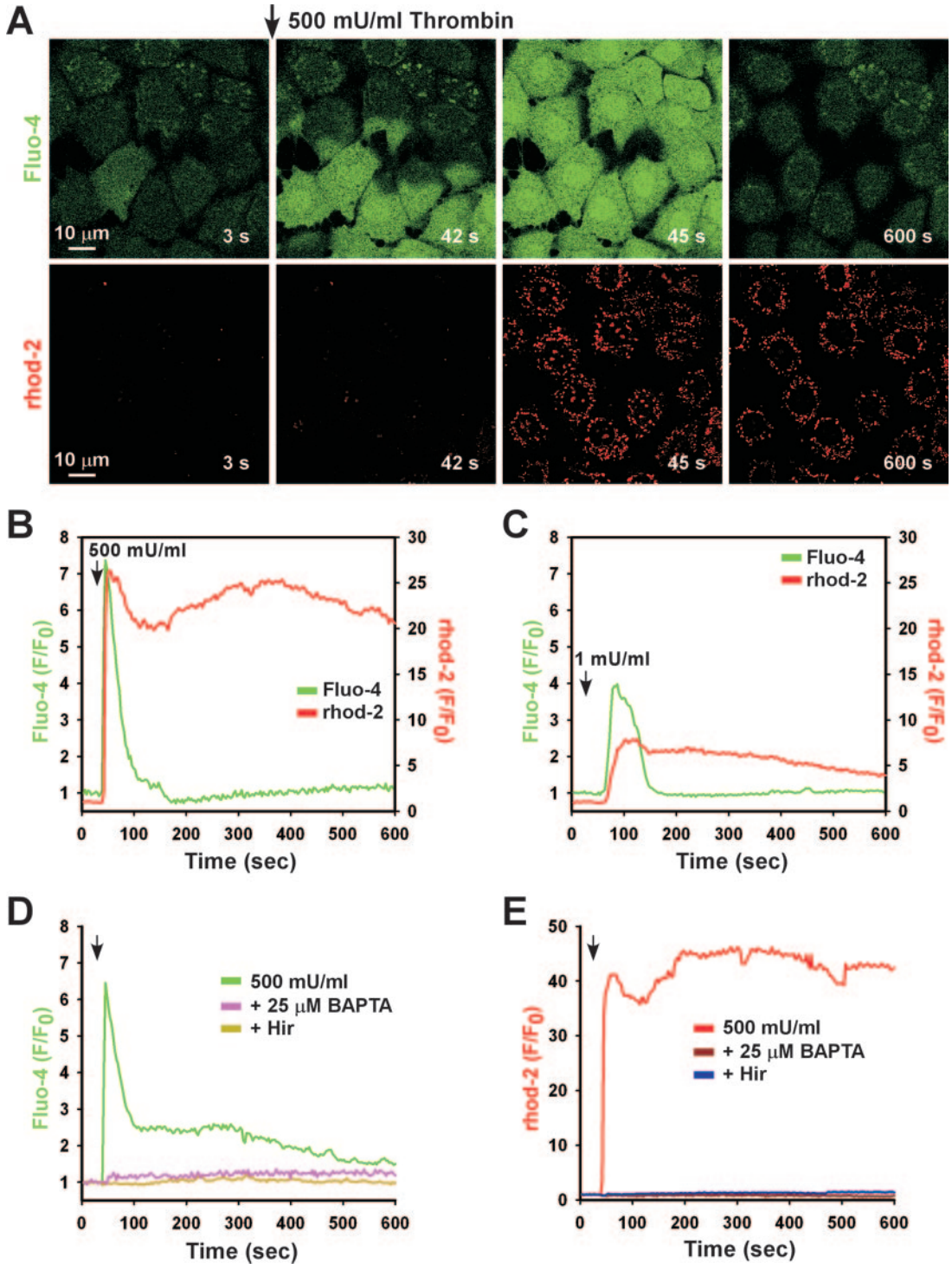

FIG. 1. Thrombin-evoked cytosolic Ca^{2+} mobilization precedes mitochondrial Ca^{2+} uptake. MPMVECs loaded with the cytosolic Ca^{2+} indicator Fluo-4/AM (green) and the mitochondrial Ca^{2+} indicator Rhod-2 (red) were stimulated with 500 mU/ml thrombin. (A) Time-lapse confocal microscopy revealed rapid Ca^{2+} mobilization, followed by mitochondrial Ca^{2+} uptake. Representative tracings of Ca^{2+} mobilization and mitochondrial Ca^{2+} uptake in response to 500 mU/ml (B) or 1 mU/ml (C) thrombin. (D and E) Inhibition of thrombin-mediated cytosolic Ca^{2+} mobilization by Hir and BAPTA abrogates mitochondrial Ca^{2+} uptake.

from stores was sufficient to trigger mROS production. The cell-permeative $O_2\cdot^-$ dismutase mimetic MnTBAP diminished mROS generation without affecting $[Ca^{2+}]_i$ mobilization (Fig. 3F). In contrast, cells stimulated in the presence of DPI had normal anti-IgM-induced Ca^{2+} mobilization as well as mROS production (Fig. 3G).

Receptor-linked mROS production does not provoke mitochondrial dysfunction. Our results demonstrate a pathway in

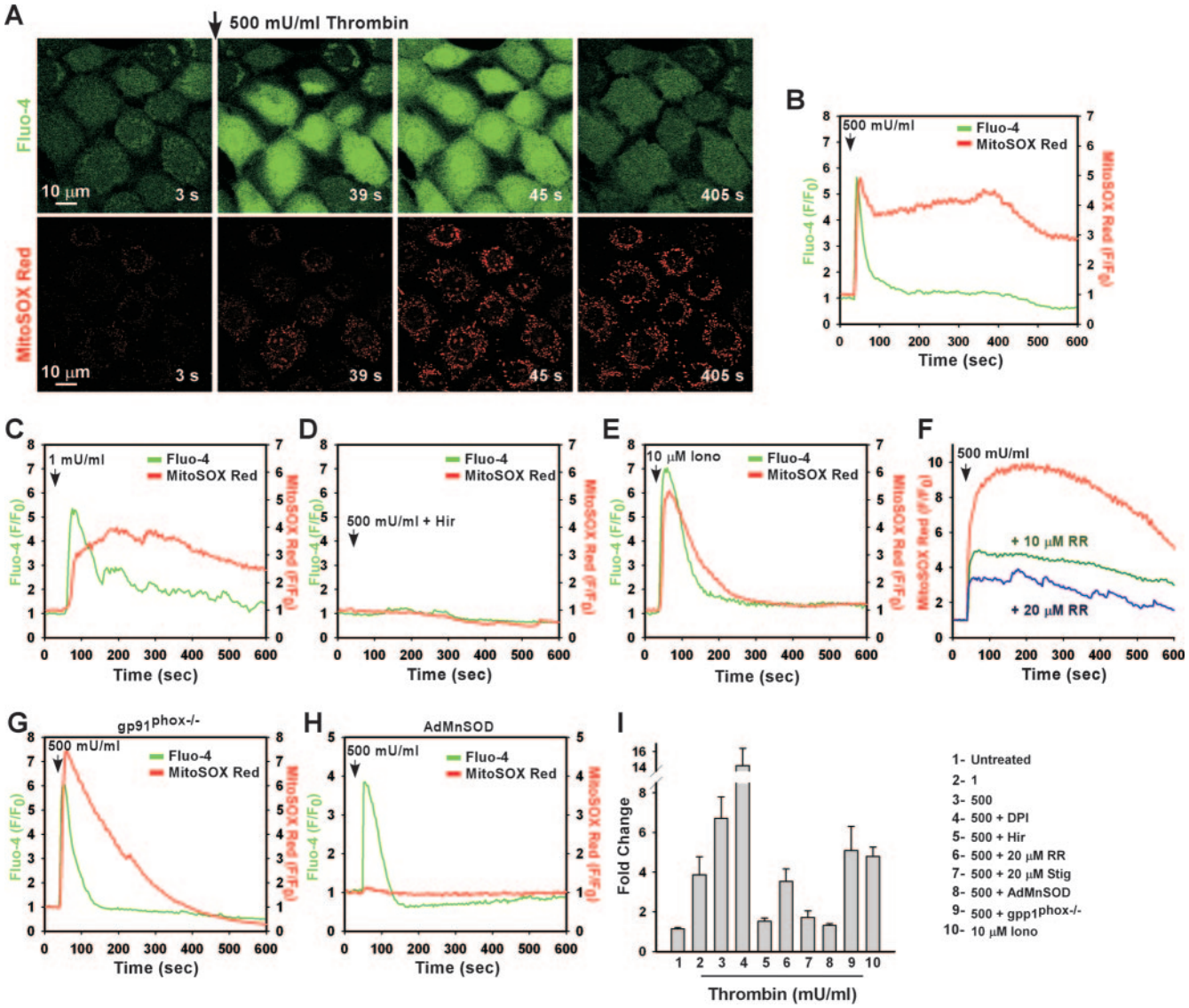

FIG. 2. Thrombin-mediated Ca^{2+} signaling stimulates mROS generation. MPMVECs loaded with Fluo-4/AM (green) and the mROS indicator MitoSOX Red (red) were stimulated with 500 mU/ml thrombin. (A) Live imaging of thrombin-evoked cytosolic Ca^{2+} mobilization and mROS production. (B to E) Representative tracings of cytosolic Ca^{2+} and mROS generation in response to 500 mU/ml (B) or 1 mU/ml (C) thrombin, 500 mU/ml thrombin plus 2 U/ml Hir (D), or 10 μM Iono (E). (F) Thrombin-induced mROS production in response to 500 mU/ml thrombin in MPMVECs pretreated with RR (10 μM or 20 μM). (G and H) mROS generation by thrombin in $gp91^{phox-/-}$ MPMVECs (G) or in MnSOD-overexpressing WT MPMVECs (H). (I) Quantitation of peak MitoSOX Red fluorescence following thrombin or Iono addition.

which agonist-induced elevations of $[Ca^{2+}]_i$ are transmitted to mitochondria, generating ROS. Previously we demonstrated that exposure of ECs to extracellular $O_2\cdot^-$ caused a mitochondrial Ca^{2+} overload that led to mitochondrial membrane depolarization and apoptosis (44). Nevertheless, PAR-mediated Ca^{2+} signaling, shown here to induce mitochondrial $O_2\cdot^-$ production, has been shown to trigger endothelial angiogenesis (64) and induce antiapoptotic gene expression (39). Paradoxically, the pattern and magnitude of the $[Ca^{2+}]_i$ transient is similar in response to both extracellular $O_2\cdot^-$ and thrombin. We therefore investigated whether PAR-triggered elevation of $[Ca^{2+}]_i$ also caused a loss of mitochondrial membrane potential ($\Delta\Psi_m$). However, thrombin-induced elevation of $[Ca^{2+}]_i$ (Fluo-4 fluorescence in Fig. 4C, D, and E) caused only small changes in $\Delta\Psi_m$. In contrast, Iono (Fig. 4A) or the SERCA pump inhibitor Tg (Fig. 4B) caused $\Delta\Psi_m$ depolarization (51). Inhibition of mitochondrial respiratory complex III by AA, which exacerbates mROS production (see Fig. S3 in the supplemental material), resulted in immediate $\Delta\Psi_m$ loss independent of $[Ca^{2+}]_i$ (Fig. 4G). These findings demonstrate that PAR-mediated cytosolic Ca^{2+} signals stimulate mitochondria to generate $O_2\cdot^-$ without leading to significant alterations in $\Delta\Psi_m$. Because excessive sequestered mitochondrial matrix Ca^{2+} as well as elevated mROS can cause mitochondrial swelling and rupture (3, 23, 25), we also examined whether receptor-mediated mitochondrial $O_2\cdot^-$ production caused structural alterations of mitochondria. However, mitochondrial size and morphology were unaltered compared to those of untreated

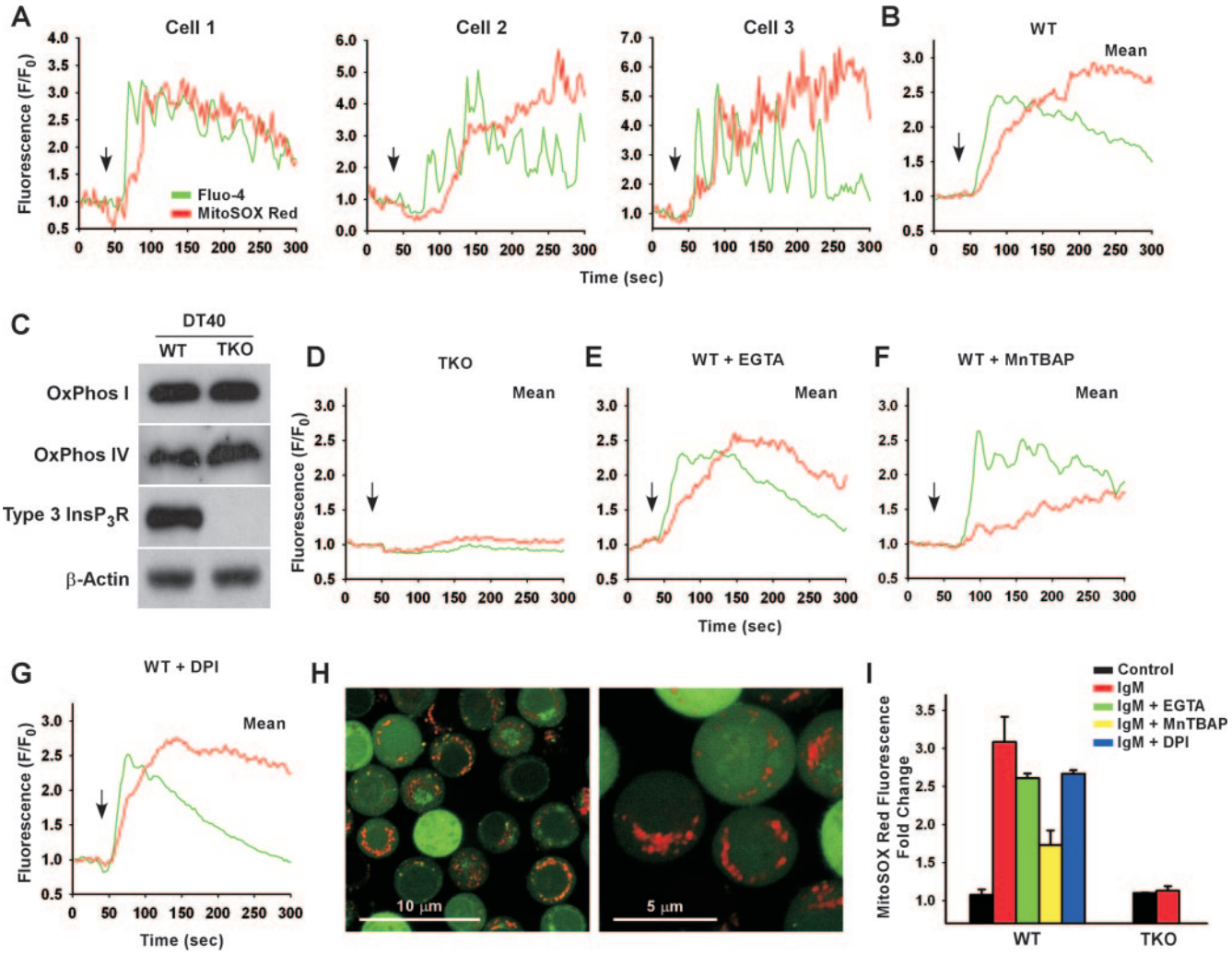

FIG. 3. BCR-mediated Ca^{2+} signaling via $InsP_3Rs$ triggers mROS production in DT40 lymphocytes. DT40 WT cells and cells lacking all three $InsP_3R$ isoforms (TKO) were loaded with Fluo-4/AM (green) and the mROS indicator MitoSOX Red (red), stimulated with 1.5 μg/ml anti-BCR antibody (anti-IgM), and simultaneously visualized for cytosolic Ca^{2+} and mROS generation. (A) Single-cell analysis of DT40 WT cells after anti-IgM cross-linking. (B) Mean increase in mROS production observed in DT40 WT cells. (C) Normal expression levels of mitochondrial complex protein I (NADH-ubiquinol oxidoreductase; OxPhos I) and complex IV (cytochrome *c* oxidase; OxPhos IV) in both DT40 WT and TKO cells. (D to G) mROS production following anti-IgM cross-linking in TKO cells (D) or WT cells in Ca^{2+}-free bath (E) or following pretreatment with the SOD mimetic MnTBAP (50 μM) (F) or DPI (10 μM) (G). (H) Low- and high-magnification images in DT40 WT cells after anti-IgM stimulation. (I) Quantitation of peak MitoSOX Red fluorescence following anti-IgM cross-linking.

cells following a 2.5-h challenge with thrombin (1.0 U/ml) (Fig. 4J). These findings indicate that thrombin-mediated mROS generation evokes neither mitochondrial membrane depolarization nor matrix swelling. Similarly, thrombin did not increase the percentage of cells that stained positive for annexin V, a marker of apoptosis (Fig. 4K and L). In contrast, extracellular $O_2\cdot^-$-mediated signaling resulted in mitochondrial depolarization (Fig. 4I) and significant cell death (Fig. 4K and L) as previously reported (44). These findings suggest that unlike paracrine-derived $O_2\cdot^-$, GPCR-mediated mROS did not lead to mitochondrial or cellular dysfunction.

GPCR-linked mitochondrial $O_2\cdot^-$ production is required for activation of inflammatory signaling. Although agonist-induced, Ca^{2+}-mediated mitochondrial $O_2\cdot^-$ production did not appear to damage ECs, it remains unknown if it might play a role in cell activation. To investigate the molecular mechanisms by which thrombin evokes endothelial activation, nuclear extracts prepared from thrombin-stimulated PMVECs were used to assess protein binding to the NF-κB consensus DNA sequence. Two distinct protein/DNA binding complexes were observed following thrombin challenge, one of which is completely abrogated by BAPTA and MnTBAP (Fig. 5A). To assess whether nuclear translocation of NF-κB complexes induces transcriptional activity, PMVECs transfected with a luciferase plasmid driven by the NF-κB promoter were stimulated with thrombin. Thrombin-mediated NF-κB transcriptional activity was absent in MnTBAP-treated PMVECs (Fig. 5B), correlating with the MnTBAP- and BAPTA-inhibitable NF-κB protein/DNA binding complex as seen in Fig. 5A. To complement the MnTBAP effect, PMVECs overexpressing

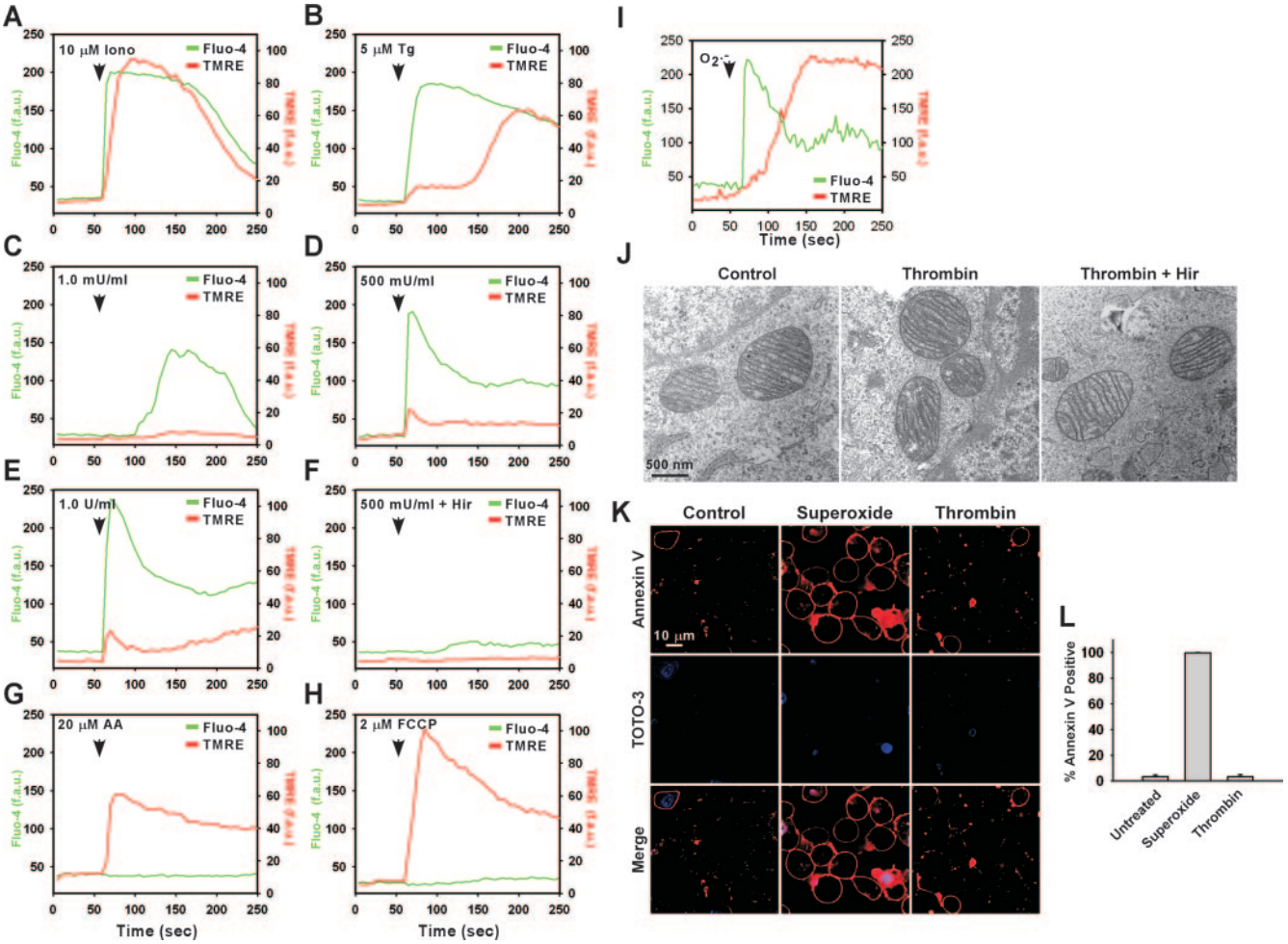

FIG. 4. Effect of thrombin-triggered Ca^{2+} signaling on mitochondrial function, morphology, and apoptosis. MPMVECs were loaded with the potentiometric dye TMRE and Fluo-4/AM (green) and imaged by confocal microscopy. Representative tracings reveal cytosolic Ca^{2+} and $\Delta\Psi_m$ in response to Iono (10 μM) (A), Tg (5 μM) (B), thrombin (1 mU/ml [C], 500 mU/ml [D], or 1,000 mU/ml [E]), or thrombin (500 mU/ml) inhibited by 2.0 U/ml Hir (F). (G and H) Increased mROS generation (complex III inhibitor AA; 20 μM) (G) or dissipation of the mitochondrial proton gradient (mitochondrial uncoupler carbonylcyanide-*p*-trifluoromethoxyphenyldrazone [FCCP]; 2 μM) (H) resulted in rapid mitochondrial depolarization independent of cytosolic Ca^{2+}. (I) Paracrine $O_2\cdot^-$ (100 μM xanthine–20 mU/ml xanthine oxidase) triggered rapid Ca^{2+} mobilization and $\Delta\Psi_m$ loss. (J) Transmission electron microscopy of untreated MPMVECs or MPMVECs following stimulation with thrombin (1 U/ml) or inactivated thrombin (2.0 U/ml Hir). (K) Annexin V and TOTO-3 staining of thrombin-treated (1 U/ml) or superoxide-treated (100 μM xanthine–20 mU/ml xanthine oxidase) MPMVECs. (L) Quantitation of percentages of annexin V-positive cells.

MnSOD also displayed an inhibition of NF-κB transcriptional activity following thrombin stimulation (Fig. 5C). The observed increase in NF-κB activity in ECs in response to PAR activation may be due to $O_2\cdot^-$ rather than other oxidants. To test this directly, PMVECs were exposed to $O_2\cdot^-$ (2 μM) or hydrogen peroxide (H_2O_2) (200 μM), and NF-κB nuclear translocation was assessed by transcription array. $O_2\cdot^-$ exposure induced an increase in NF-κB activity in PMVECs that was absent in H_2O_2-treated cells, suggesting a discrete role for $O_2\cdot^-$ in endothelial cell activation (see Figure S5 in the supplemental material).

The role of ROS in NF-κB activation is controversial (29) and is commonly evaluated in response to proinflammatory molecules such as TNF-α (6). PMVECs stimulated with TNF-α exhibited significant NF-κB activity that was not inhibited by MnTBAP, indicating that TNF-α-mediated NF-κB activity is independent of mitochondrial $O_2\cdot^-$ production (Fig. 5B). To distinguish the role of GPCR-linked physiological versus nonphysiological mitochondrial $O_2\cdot^-$ signaling, we next determined whether AA-induced ROS could also lead to NF-κB transcriptional activity. In contrast to thrombin, mROS production by AA did not trigger either NF-κB DNA binding (Fig. 5A) or transcriptional activity (Fig. 5B). Since AA but not thrombin facilitates $\Delta\Psi_m$ loss (Fig. 4G and E, respectively), we next asked whether AA leads to mitochondrial $O_2\cdot^-$ overproduction. AA results in dramatic mitochondrial $O_2\cdot^-$ production compared to thrombin-mediated physiologic signaling (Fig. 5D and E). Together with NF-κB activity and $\Delta\Psi_m$ measurement, these data indicate that physiologic $O_2\cdot^-$ production is required for NF-κB-mediated signaling.

TNF-α and shear stress induce ICAM-1 expression by NF-κB activation in ECs (32, 50). Thrombin strongly induced

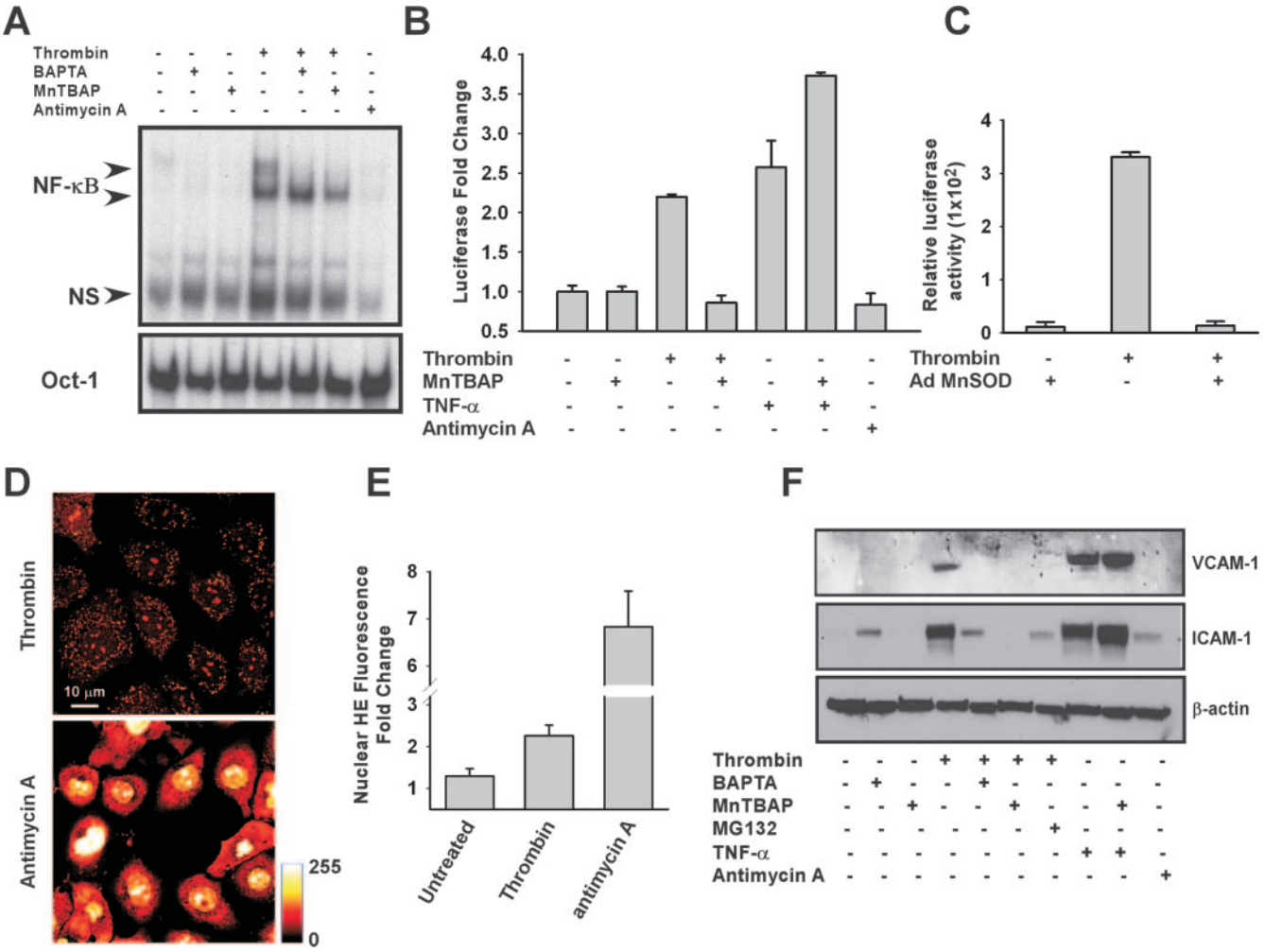

FIG. 5. Activation of NF-κB and expression of ICAM-1 by GPCR-linked mROS. (A) Protein binding to the NF-κB consensus sequence following thrombin stimulation in the presence or absence of BAPTA and MnTBAP. (B) NF-κB transcriptional activity in response to thrombin or TNF-α (10 ng/ml) as assessed by luciferase reporter assay. Luciferase reporter constructs were normalized to β-galactosidase activity. (C) Overexpression of MnSOD abolished thrombin-induced NF-κB activity. (D) Global $O_2\cdot^-$ production is assessed by HE fluorescence in response to both thrombin (500 mU/ml) and AA (20 μM) following 10 min of stimulation. (E) Quantitation of nuclear HE fluorescence increase in response to AA and thrombin. (F) VCAM-1 and ICAM-1 expression following thrombin or TNF-α stimulation in the presence of MnTBAP (50 μM), BAPTA (25 μM), or the proteosomal inhibitor MG132 in HPMVECs.

ICAM-1 expression to a level comparable to that of TNF-α. In contrast, thrombin triggered only a nominal induction in VCAM-1 expression compared to that of TNF-α (Fig. 5F). The proteosomal inhibitor MG132 (3 μM), which inhibits degradation of the NF-κB inhibitory IκB protein, blocked thrombin-induced ICAM-1 expression, indicating that the response is NF-κB dependent (Fig. 5F). Remarkably, ICAM-1 induction was completely abrogated by the $O_2\cdot^-$ dismutase mimetic MnTBAP. In contrast, MnTBAP was without effect on either baseline ICAM-1 expression or thrombin-mediated $[Ca^{2+}]_i$ signaling (see Fig. S6 in the supplemental material). Similarly, BAPTA pretreatment abrogated thrombin-mediated ICAM-1 upregulation. Notably, TNF-α-triggered ICAM-1 induction was not affected by MnTBAP pretreatment. In contrast to that of ICAM-1, expression of VCAM-1 was greatly induced by TNF-α but not thrombin (Fig. 5F). These results indicate that thrombin-linked NF-κB activation drives ICAM-1 expression and is dependent on physiological mitochondrial $O_2\cdot^-$ production.

Receptor-linked mitochondrial $O_2\cdot^-$ production evokes leukocyte/EC firm adhesion. Enhanced expression of ICAM-1 and VCAM-1 but not ICAM-2 facilitates binding of leukocytes to activated ECs (33, 56). To determine the functional relevance of GPCR-linked mROS-dependent ICAM-1 expression, we performed live cell confocal microscopy to image leukocyte/EC interactions in a simulated circulation model. Under quiescent conditions, flow disrupted the adhesion between ECs and leukocytes (Fig. 6A and B), whereas HPMVECs challenged with thrombin (500 mU/ml) demonstrated rapid and massive leukocyte/EC firm adhesion. Remarkably, pretreatment of ECs with the $O_2\cdot^-$ dismutase mimetic MnTBAP (50 μM) or overexpression of the mitochondrial SOD isoform inhibited thrombin-induced firm adhesion of leukocytes to HPMVECs. Further, an anti-ICAM-1 blocking antibody also dis-

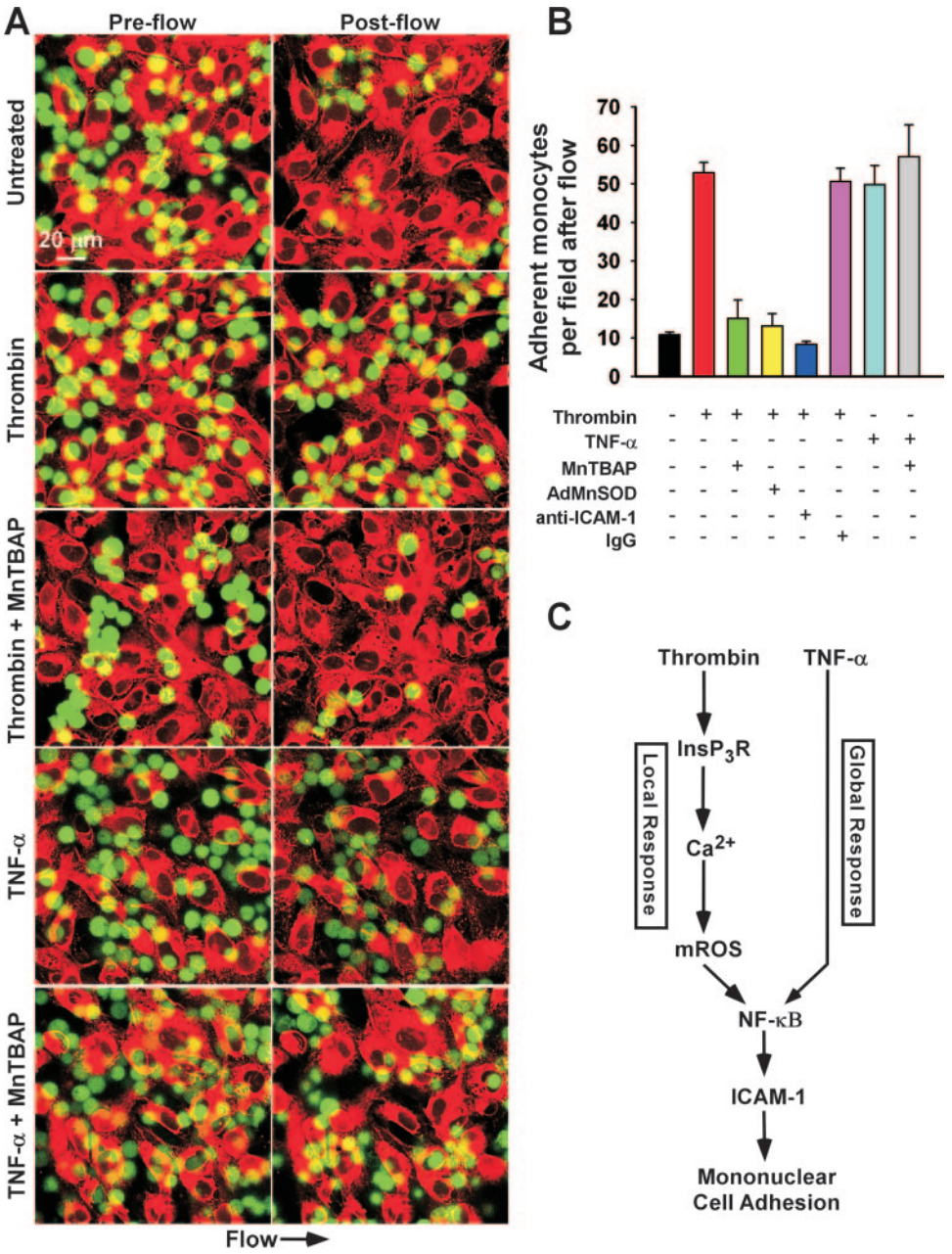

FIG. 6. Thrombin-mediated mROS is requisite for leukocyte firm adherence via ICAM-1. Cell Tracker Red-labeled HPMVECs were treated with thrombin (500 mU/ml) or TNF-α (10 ng/ml) with or without MnTBAP (50 μM) pretreatment. An equivalent number of Cell Tracker Green-labeled J774.1 macrophages were added to HPMVECs for each experiment and subjected to simulated circulation to assess leukocyte firm adhesion. (A) Live cell images were acquired under high-power field via confocal microscopy prior to and following 6 min of 2.5 dynes/cm^2 shear stress. (B) Quantitation of adherent leukocytes following thrombin or TNF-α challenge in the absence or presence of MnTBAP. Thrombin-mediated leukocyte/EC binding was effectively reduced by MnTBAP, overexpression of MnSOD, and an anti-ICAM-1 blocking antibody. (C) Proposed model of local versus global leukocyte/EC firm adhesion following GPCR-linked mROS production and TNFR signaling, respectively.

rupted leukocyte/EC adhesion, suggesting that thrombin-mediated mROS production and consequent ICAM-1 induction is critical for leukocyte firm adhesion. In contrast, TNF-α also produced significant leukocyte/EC firm adhesion (Fig. 5B), but mROS was not required (see Fig. S7 in the supplemental material). Overall, these results demonstrate that GPCR-linked mROS production is essential for ICAM-1 expression and leukocyte/EC firm adhesion.

DISCUSSION

In this study we have identified GPCR-linked mitochondrial $O_2{\cdot}^-$ production as an important signaling system that plays a critical role in leukocyte adhesion to the vascular endothelium. The GPCR agonist thrombin mobilizes Ca^{2+} via $InsP_3R$, raises mitochondrial Ca^{2+} levels, and causes mROS production. mROS generated by this pathway activates NF-κB signaling,

strongly induces the expression of ICAM-1, and promotes the adhesion of nonactivated leukocytes to the vascular endothelium. These effects are specific to $O_2\cdot^-$ generated by mitochondria, since NADPH oxidase is dispensable for endothelial activation. Thus, mROS is not simply a by-product of mitochondrial respiration but is rather a key factor that "decodes" $InsP_3R$-induced Ca^{2+} signals in ECs into ICAM-1-mediated leukocyte adherence.

ROS are increasingly associated with both pathological and physiologic cell signaling (20, 44, 59). Cells generate ROS through a variety of sources, including but not limited to NADPH oxidase, xanthine oxidase, and the mitochondrial electron transport chain. Extracellular ROS produced by NADPH oxidase has been implicated in cellular proliferation (18) and endothelial inflammation (54). NADPH oxidase has also been invoked to account for intracellular ROS production (61) despite the fact that the enzyme functions to produce extracellular $O_2\cdot^-$ (37). It is conceivable that in many instances in which intracellular ROS is implicated in physiological regulation, the source is not NADPH oxidase. Although ECs are considered primarily glycolytic in nature (53), mitochondria are a likely source of ROS since ECs are laden with mitochondria (13). In this study, we demonstrate that leukocyte adherence to ECs is stimulated in GPCR-activated ECs and that the rapid firm adherence involves EC mROS specifically.

This unique role for mROS in thrombin-mediated EC activation is supported by several lines of evidence. Thrombin elicited a large $[Ca^{2+}]_i$ transient in ECs that was followed by mitochondrion-specific $O_2\cdot^-$ production, as assessed by MitoSOX Red staining. This $O_2\cdot^-$ was likely produced as a by-product of increased mitochondrial respiration by activated cells (22, 58), since cells lacking a functional NADPH oxidase complex ($gp91^{phox-/-}$) still produced mitochondrial $O_2\cdot^-$ during GPCR signaling. mROS production was triggered by a rise of mitochondrial Ca^{2+} derived from the endoplasmic reticulum, since it was abolished in a cell line lacking $InsP_3R$, and it was reduced by pharmacologic inhibition of mitochondrial Ca^{2+} uptake. Further, elimination of extracellular Ca^{2+} did not appreciably inhibit mROS production, underscoring that Ca^{2+} release, and not subsequent Ca^{2+} influx from the extracellular environment, is critical for mROS-mediated signaling. Whereas mROS production was prevented by MnSOD overexpression, MnSOD had no effect on GPCR-linked Ca^{2+} signaling, indicating that mROS production is downstream of $InsP_3R$-mediated Ca^{2+} release. mROS was generated in response to both GPCR and tyrosine kinase receptor cascades in ECs and hematopoietic cells, respectively, indicating that the response may represent a common mechanism linking $InsP_3R$-triggered cellular activation to inflammation (30) and possibly other Ca^{2+}-regulated cell physiological processes. NF-κB is involved in various signaling pathways, including cell survival, differentiation, and even apoptosis (12). Our data clearly demonstrate that NF-κB activation is downstream of Ca^{2+} mobilization and mROS production. Activation of NF-κB by Ca^{2+}-mediated mROS production may therefore constitute a mechanism by which varied cell signaling pathways, including angiotensin II (19) and vascular endothelial growth factor (16), converge at the mitochondrion to elicit similar cellular outcomes via NF-κB-induced gene expression. Our study demonstrates that mROS is a downstream effector molecule that decodes a GPCR-mediated Ca^{2+} signal. Paracrine-derived ROS causes cellular dysfunction and mitochondrion-dependent apoptosis (44). However, thrombin-enhanced mROS production did not cause either mitochondrial dysfunction or apoptosis (Fig. 4). Thus, the cellular responses to receptor-mediated mROS production are distinct from those elicited by paracrine-derived ROS. The results from this study suggest that acute Ca^{2+} signals may be translated into physiological signals via mROS. In the model described here, GPCR-linked mROS production induced inflammatory signaling via NF-κB and subsequent proinflammatory molecule expression that enhanced leukocyte/EC adhesion.

The transcription factor NF-κB is activated in response to varied inflammatory stimuli and results in altered gene and protein expression and endothelial activation (62). Many of these stimuli increase ROS production, leading to the early hypothesis that NF-κB was controlled by elevated cellular ROS (1), of which H_2O_2 was considered the most likely species (38). However, it is becoming clear from the available data that H_2O_2-induced NF-κB activation is highly cell type dependent and therefore H_2O_2 is unlikely to be a general mediator of NF-κB activation (29). Our studies represent a novel mechanism whereby mitochondrial Ca^{2+}-triggered $O_2\cdot^-$, rather than H_2O_2, is the key component of the cellular response to inflammatory stimuli. In support, $O_2\cdot^-$ but not H_2O_2 elicited NF-κB translocation in ECs. Further, both MnSOD overexpression and MnTBAP completely abrogated NF-κB transcriptional activity and downstream protein expression. This response was specific for receptor-mediated mROS, since mROS overproduction led to mitochondrial dysfunction and did not induce NF-κB activation or drive ICAM-1 expression. We suggest that overproduction of mROS may lead to inactivation of NF-κB, mitochondrial dysfunction, and cell death.

EC activation by cytokines results in the induction of cell adhesion molecules such as ICAM-1, VCAM-1, and E-selectin (17, 21). ICAM-1 is vital for the adherence and transmigration of leukocytes on the endothelium (40, 46, 56, 57). ICAM-1 can also be induced by cytokine-independent mechanisms during ischemia/reperfusion, angiogenesis, and thrombin challenge (7, 35, 54). Cytokine-induced EC expression of adhesion molecules has been shown to be dependent on *N*-acetylcysteine-inhibitable oxidative events (45). However, the oxidant that controls adhesion molecule expression and its cellular source is unknown. Our studies have identified a mechanism in which GPCR Ca^{2+} signals are translated into mROS, which upregulates the expression of ICAM-1 via NF-κB and elicits leukocyte/EC firm adhesion. It appears likely therefore that mitochondria are the ROS source responsible for endothelial activation in response to GPCR signals. While Ca^{2+} signaling in leukocytes is not involved in endothelial firm adhesion (24), we establish here that Ca^{2+}-linked mROS production in ECs is required for leukocyte/EC firm adhesion.

This study demonstrates a unique mechanism in which GPCR-linked mROS production enhances leukocyte adhesion to the activated endothelium without affecting leukocyte signaling (unpublished data). On the other hand, proinflammatory cytokines such as TNF-α activate both leukocytes and ECs and facilitate leukocyte/EC firm adhesion in an mROS-independent manner (Fig. 6C). That these two major signals both trigger leukocyte/EC firm adhesion by divergent mechanisms

demonstrates a fundamental difference between GPCR and TNFR signaling. Indeed, in contrast to GPCR signaling, ROS does not appear to have a role in NF-κB activation and subsequent ICAM-1 expression in TNFR-mediated signaling. Furthermore, the event underlying thrombin-induced EC activation provides a mechanism for local regulation of leukocyte/EC interactions. First, thrombin is released locally from activated platelets to rapidly facilitate clot formation and endothelial wound healing via recruitment of circulating leukocytes (41). Second, the short lifetime of mROS (μs) ensures that its signaling remains highly localized. We postulate that the transient nature of mROS locally restricts the actions of thrombin, in contrast to the effects of proinflammatory cytokines that globally sensitize both leukocytes and the vasculature (Fig. 6C). Atherosclerosis and hypertension are associated with elevated thrombin in the circulation (60). Our results suggest that in this context, elevated thrombin-mediated mROS production throughout the vasculature could cause global endothelial activation that leads to disease progression.

The findings of this study provide experimental and mechanistic evidence for GPCR-linked Ca^{2+}-stimulated physiological mROS production in leukocyte/EC firm adhesion. They may also offer a mechanistic explanation for thrombin-induced vascular inflammation. Future studies using in vivo models may reveal the implications of these results for the progression and treatment of vascular diseases, including the use of antioxidant therapy for patients with elevated circulating thrombin levels.

ACKNOWLEDGMENTS

We thank T. Kurosaki for DT40 cells, Craig B. Thompson, Aron B. Fisher, Gyorgy Hajnoczky, and Russell Jones for their helpful thoughts and suggestions, Kevin Yu for electron microscopy studies, Kris DeBolt and Atsuko Kataoka for cell isolation and culture, and Lijuan Mei for Western blot analysis. We gratefully acknowledge John F. Engelhardt and the Vector Facility of the University of Iowa for the AdMnSOD construct.

This work was supported by an AHA Scientist Development Grant and University Research Foundation award to M.M., SDG 0435284 to M.R.A., and NIH grant GM/DK56328 to J.K.F. Brian Hawkins was supported by a postdoctoral fellowship from the Pulmonary Hypertension Association.

REFERENCES

1. **Baeuerle, P. A., and T. Henkel.** 1994. Function and activation of NF-kappa B in the immune system. Annu. Rev. Immunol. **12:**141–179.
2. **Bell, E. L., T. A. Klimova, J. Eisenbart, C. T. Moraes, M. P. Murphy, G. R. Budinger, and N. S. Chandel.** 2007. The Qo site of the mitochondrial complex III is required for the transduction of hypoxic signaling via reactive oxygen species production. J. Cell Biol. **177:**1029–1036.
3. **Bernardi, P., L. Scorrano, R. Colonna, V. Petronilli, and F. Di Lisa.** 1999. Mitochondria and cell death. Mechanistic aspects and methodological issues. Eur. J. Biochem. **264:**687–701.
4. **Berridge, M. J., M. D. Bootman, and P. Lipp.** 1998. Calcium—a life and death signal. Nature **395:**645–648.
5. **Berridge, M. J., M. D. Bootman, and H. L. Roderick.** 2003. Calcium signalling: dynamics, homeostasis and remodelling. Nat. Rev. Mol. Cell Biol. **4:**517–529.
6. **Bubici, C., S. Papa, K. Dean, and G. Franzoso.** 2006. Mutual cross-talk between reactive oxygen species and nuclear factor-kappa B: molecular basis and biological significance. Oncogene **25:**6731–6748.
7. **Burne, M. J., A. Elghandour, M. Haq, S. R. Saba, J. Norman, T. Condon, F. Bennett, and H. Rabb.** 2001. IL-1 and TNF independent pathways mediate ICAM-1/VCAM-1 up-regulation in ischemia reperfusion injury. J. Leukoc. Biol. **70:**192–198.
8. **Campbell, J. J., and E. C. Butcher.** 2000. Chemokines in tissue-specific and microenvironment-specific lymphocyte homing. Curr. Opin. Immunol. **12:** 336–341.
9. **Carlos, T. M., R. S. Clark, D. Franicola-Higgins, J. K. Schiding, and P. M. Kochanek.** 1997. Expression of endothelial adhesion molecules and recruitment of neutrophils after traumatic brain injury in rats. J. Leukoc. Biol. **61:**279–285.
10. **Castilho, R. F., O. Hansson, M. W. Ward, S. L. Budd, and D. G. Nicholls.** 1998. Mitochondrial control of acute glutamate excitotoxicity in cultured cerebellar granule cells. J. Neurosci. **18:**10277–10286.
11. **Cinamon, G., V. Shinder, and R. Alon.** 2001. Shear forces promote lymphocyte migration across vascular endothelium bearing apical chemokines. Nat. Immunol. **2:**515–522.
12. **Claudio, E., K. Brown, and U. Siebenlist.** 2006. NF-κB guides the survival and differentiation of developing lymphocytes. Cell Death Differ. **13:**697–701.
13. **Collins, T. J., M. J. Berridge, P. Lipp, and M. D. Bootman.** 2002. Mitochondria are morphologically and functionally heterogeneous within cells. EMBO J. **21:**1616–1627.
14. **Coughlin, S. R.** 2005. Protease-activated receptors in hemostasis, thrombosis and vascular biology. J. Thromb. Haemost. **3:**1800–1814.
15. **Coughlin, S. R.** 2000. Thrombin signalling and protease-activated receptors. Nature **407:**258–264.
16. **Dawson, N. S., D. C. Zawieja, M. H. Wu, and H. J. Granger.** 2006. Signaling pathways mediating VEGF165-induced calcium transients and membrane depolarization in human endothelial cells. FASEB J. **20:**991–993.
17. **Dejana, E., F. Bertocchi, M. C. Bortolami, A. Regonesi, A. Tonta, F. Breviario, and R. Giavazzi.** 1988. Interleukin 1 promotes tumor cell adhesion to cultured human endothelial cells. J. Clin. Investig. **82:**1466–1470.
18. **Devadas, S., L. Zaritskaya, S. G. Rhee, L. Oberley, and M. S. Williams.** 2002. Discrete generation of superoxide and hydrogen peroxide by T cell receptor stimulation: selective regulation of mitogen-activated protein kinase activation and fas ligand expression. J. Exp. Med. **195:**59–70.
19. **Douillette, A., A. Bibeau-Poirier, S. P. Gravel, J. F. Clement, V. Chenard, P. Moreau, and M. J. Servant.** 2006. The proinflammatory actions of angiotensin II are dependent on p65 phosphorylation by the IκB kinase complex. J. Biol. Chem. **281:**13275–13284.
20. **Droge, W.** 2002. Free radicals in the physiological control of cell function. Physiol. Rev. **82:**47–95.
21. **Dustin, M. L., and T. A. Springer.** 1991. Role of lymphocyte adhesion receptors in transient interactions and cell locomotion. Annu. Rev. Immunol. **9:**27–66.
22. **Esposito, L. A., S. Melov, A. Panov, B. A. Cottrell, and D. C. Wallace.** 1999. Mitochondrial disease in mouse results in increased oxidative stress. Proc. Natl. Acad. Sci. USA **96:**4820–4825.
23. **Galindo, M. F., J. Jordan, C. Gonzalez-Garcia, and V. Cena.** 2003. Reactive oxygen species induce swelling and cytochrome c release but not transmembrane depolarization in isolated rat brain mitochondria. Br. J. Pharmacol. **139:**797–804.
24. **Gerszten, R. E., E. A. Garcia-Zepeda, Y. C. Lim, M. Yoshida, H. A. Ding, M. A. Gimbrone, Jr., A. D. Luster, F. W. Luscinskas, and A. Rosenzweig.** 1999. MCP-1 and IL-8 trigger firm adhesion of monocytes to vascular endothelium under flow conditions. Nature **398:**718–723.
25. **Giorgio, M., E. Migliaccio, F. Orsini, D. Paolucci, M. Moroni, C. Contursi, G. Pelliccia, L. Luzi, S. Minucci, M. Marcaccio, P. Pinton, R. Rizzuto, P. Bernardi, F. Paolucci, and P. G. Pelicci.** 2005. Electron transfer between cytochrome c and p66Shc generates reactive oxygen species that trigger mitochondrial apoptosis. Cell **122:**221–233.
26. **Hajnoczky, G., L. D. Robb-Gaspers, M. B. Seitz, and A. P. Thomas.** 1995. Decoding of cytosolic calcium oscillations in the mitochondria. Cell **82:**415–424.
27. **Han, D., F. Antunes, R. Canali, D. Rettori, and E. Cadenas.** 2003. Voltage-dependent anion channels control the release of the superoxide anion from mitochondria to cytosol. J. Biol. Chem. **278:**5557–5563.
28. **Hawkins, B. J., M. Madesh, C. J. Kirkpatrick, and A. B. Fisher.** 2007. Superoxide flux in endothelial cells via the chloride channel-3 mediates intracellular signaling. Mol. Biol. Cell **18:**2002–2012.
29. **Hayakawa, M., H. Miyashita, I. Sakamoto, M. Kitagawa, H. Tanaka, H. Yasuda, M. Karin, and K. Kikugawa.** 2003. Evidence that reactive oxygen species do not mediate NF-κB activation. EMBO J. **22:**3356–3366.
30. **Hensley, K., K. A. Robinson, S. P. Gabbita, S. Salsman, and R. A. Floyd.** 2000. Reactive oxygen species, cell signaling, and cell injury. Free Radic. Biol. Med. **28:**1456–1462.
31. **Jacobson, J., and M. R. Duchen.** 2004. Interplay between mitochondria and cellular calcium signalling. Mol. Cell. Biochem. **257:**209–218.
32. **Johnson, D. R., I. Douglas, A. Jahnke, S. Ghosh, and J. S. Pober.** 1996. A sustained reduction in IκB-β may contribute to persistent NF-κB activation in human endothelial cells. J. Biol. Chem. **271:**16317–16322.
33. **Johnson, L. A., S. Clasper, A. P. Holt, P. F. Lalor, D. Baban, and D. G. Jackson.** 2006. An inflammation-induced mechanism for leukocyte transmigration across lymphatic vessel endothelium. J. Exp. Med. **203:**2763–2777.
34. **Kataoka, H., J. R. Hamilton, D. D. McKemy, E. Camerer, Y. W. Zheng, A. Cheng, C. Griffin, and S. R. Coughlin.** 2003. Protease-activated receptors 1 and 4 mediate thrombin signaling in endothelial cells. Blood **102:**3224–3231.
35. **Kim, I., S. O. Moon, S. H. Kim, H. J. Kim, Y. S. Koh, and G. Y. Koh.** 2001. Vascular endothelial growth factor expression of intercellular adhesion molecule 1 (ICAM-1), vascular cell adhesion molecule 1 (VCAM-1), and E-

selectin through nuclear factor-kappa B activation in endothelial cells. J. Biol. Chem. **276:**7614–7620.
36. **Kirichok, Y., G. Krapivinsky, and D. E. Clapham.** 2004. The mitochondrial calcium uniporter is a highly selective ion channel. Nature **427:**360–364.
37. **Lambeth, J. D.** 2004. NOX enzymes and the biology of reactive oxygen. Nat. Rev. Immunol. **4:**181–189.
38. **Li, N., and M. Karin.** 1999. Is NF-κB the sensor of oxidative stress? FASEB J. **13:**1137–1143.
39. **Ludeman, M. J., H. Kataoka, Y. Srinivasan, N. L. Esmon, C. T. Esmon, and S. R. Coughlin.** 2005. PAR1 cleavage and signaling in response to activated protein C and thrombin. J. Biol. Chem. **280:**13122–13128.
40. **Luscinskas, F. W., M. I. Cybulsky, J. M. Kiely, C. S. Peckins, V. M. Davis, and M. A. Gimbrone, Jr.** 1991. Cytokine-activated human endothelial monolayers support enhanced neutrophil transmigration via a mechanism involving both endothelial-leukocyte adhesion molecule-1 and intercellular adhesion molecule-1. J. Immunol. **146:**1617–1625.
41. **Ma, L., R. Perini, W. McKnight, M. Dicay, A. Klein, M. D. Hollenberg, and J. L. Wallace.** 2005. Proteinase-activated receptors 1 and 4 counter-regulate endostatin and VEGF release from human platelets. Proc. Natl. Acad. Sci. USA **102:**216–220.
42. **Macfarlane, S. R., M. J. Seatter, T. Kanke, G. D. Hunter, and R. Plevin.** 2001. Proteinase-activated receptors. Pharmacol. Rev. **53:**245–282.
43. **Madesh, M., and G. Hajnoczky.** 2001. VDAC-dependent permeabilization of the outer mitochondrial membrane by superoxide induces rapid and massive cytochrome c release. J. Cell Biol. **155:**1003–1015.
44. **Madesh, M., B. J. Hawkins, T. Milovanova, C. D. Bhanumathy, S. K. Joseph, S. P. Ramachandrarao, K. Sharma, T. Kurosaki, and A. B. Fisher.** 2005. Selective role for superoxide in InsP3 receptor-mediated mitochondrial dysfunction and endothelial apoptosis. J. Cell Biol. **170:**1079–1090.
45. **Marui, N., M. K. Offermann, R. Swerlick, C. Kunsch, C. A. Rosen, M. Ahmad, R. W. Alexander, and R. M. Medford.** 1993. Vascular cell adhesion molecule-1 (VCAM-1) gene transcription and expression are regulated through an antioxidant-sensitive mechanism in human vascular endothelial cells. J. Clin. Investig. **92:**1866–1874.
46. **Meerschaert, J., and M. B. Furie.** 1995. The adhesion molecules used by monocytes for migration across endothelium include CD11a/CD18, CD11b/CD18, and VLA-4 on monocytes and ICAM-1, VCAM-1, and other ligands on endothelium. J. Immunol. **154:**4099–4112.
47. **Milovanova, T., S. Chatterjee, Y. Manevich, I. Kotelnikova, K. Debolt, M. Madesh, J. S. Moore, and A. B. Fisher.** 2006. Lung endothelial cell proliferation with decreased shear stress is mediated by reactive oxygen species. Am. J. Physiol. Cell Physiol. **290:**C66–C76.
48. **Mukhopadhyay, P., M. Rajesh, K. Yoshihiro, G. Hasko, and P. Pacher.** 2007. Simple quantitative detection of mitochondrial superoxide production in live cells. Biochem. Biophys. Res. Commun. **358:**203–208.
49. **Muller, F. L., Y. Liu, and H. Van Remmen.** 2004. Complex III releases superoxide to both sides of the inner mitochondrial membrane. J. Biol. Chem. **279:**49064–49073.
50. **Orr, A. W., J. M. Sanders, M. Bevard, E. Coleman, I. J. Sarembock, and M. A. Schwartz.** 2005. The subendothelial extracellular matrix modulates NF-κB activation by flow: a potential role in atherosclerosis. J. Cell Biol. **169:**191–202.
51. **Pacher, P., and G. Hajnoczky.** 2001. Propagation of the apoptotic signal by mitochondrial waves. EMBO J. **20:**4107–4121.
52. **Parekh, A. B., and J. W. Putney, Jr.** 2005. Store-operated calcium channels. Physiol. Rev. **85:**757–810.
53. **Quintero, M., S. L. Colombo, A. Godfrey, and S. Moncada.** 2006. Mitochondria as signaling organelles in the vascular endothelium. Proc. Natl. Acad. Sci. USA **103:**5379–5384.
54. **Rahman, A., K. N. Anwar, S. Uddin, N. Xu, R. D. Ye, L. C. Platanias, and A. B. Malik.** 2001. Protein kinase C-δ regulates thrombin-induced ICAM-1 gene expression in endothelial cells via activation of p38 mitogen-activated protein kinase. Mol. Cell. Biol. **21:**5554–5565.
55. **Rizzuto, R., P. Pinton, W. Carrington, F. S. Fay, K. E. Fogarty, L. M. Lifshitz, R. A. Tuft, and T. Pozzan.** 1998. Close contacts with the endoplasmic reticulum as determinants of mitochondrial Ca2+ responses. Science **280:**1763–1766.
56. **Schenkel, A. R., Z. Mamdouh, and W. A. Muller.** 2004. Locomotion of monocytes on endothelium is a critical step during extravasation. Nat. Immunol. **5:**393–400.
57. **Springer, T. A.** 1994. Traffic signals for lymphocyte recirculation and leukocyte emigration: the multistep paradigm. Cell **76:**301–314.
58. **Starkov, A. A., C. Chinopoulos, and G. Fiskum.** 2004. Mitochondrial calcium and oxidative stress as mediators of ischemic brain injury. Cell Calcium **36:**257–264.
59. **Storz, P., H. Doppler, and A. Toker.** 2005. Protein kinase D mediates mitochondrion-to-nucleus signaling and detoxification from mitochondrial reactive oxygen species. Mol. Cell. Biol. **25:**8520–8530.
60. **Tracy, R. P.** 2003 Thrombin, inflammation, and cardiovascular disease: an epidemiologic perspective. Chest **124:**49S–57S.
61. **Ushio-Fukai, M.** 2006. Localizing NADPH oxidase-derived ROS. Sci. STKE **2006:**re8.
62. **Wada, Y., H. Otu, S. Wu, M. R. Abid, H. Okada, T. Libermann, T. Kodama, S. C. Shih, T. Minami, and W. C. Aird.** 2005. Preconditioning of primary human endothelial cells with inflammatory mediators alters the "set point" of the cell. FASEB J. **19:**1914–1916.
63. **White, C., C. Li, J. Yang, N. B. Petrenko, M. Madesh, C. B. Thompson, and J. K. Foskett.** 2005. The endoplasmic reticulum gateway to apoptosis by Bcl-X(L) modulation of the InsP3R. Nat. Cell Biol. **7:**1021–1028.
64. **Zania, P., S. Kritikou, C. S. Flordellis, M. E. Maragoudakis, and N. E. Tsopanoglou.** 2006. Blockade of angiogenesis by small molecule antagonists to protease-activated receptor-1: association with endothelial cell growth suppression and induction of apoptosis. J. Pharmacol. Exp. Ther. **318:**246–254.